Hydrogen Bond Network in the Distal Site of Peroxidases: Spectroscopic Properties of Asn70 → Asp Horseradish Peroxidase Mutant†

Motomasa Tanaka, Shingo Nagano,‡ Koichiro Ishimori, and Isao Morishima*

Department of Molecular Engineering, Graduate School of Engineering, Kyoto University, Kyoto 606-01, Japan

Received March 18, 1997; Revised Manuscript Received May 22, 1997⊗

ABSTRACT: The distal His in peroxidases forms a hydrogen bond with the adjacent Asn, which is highly conserved among many plant and fungal peroxidases. Our previous work [Nagano, S., Tanaka, M., Ishimori, K., Watanabe, Y., & Morishima, I. (1996) *Biochemistry 35*, 14251−14258] has revealed that the replacement of Asn70 in horseradish peroxidase C (HRP) by Val (N70V) and Asp (N70D) discourages the oxidation activity for guaiacol, and the elementary reaction rate constants for the mutants was decreased by 10−15-fold. In order to delineate the structure−function relationship of the His−Asn couple in peroxidase activity, heme environmental structures of the HRP mutant, N70D, were investigated by CD, ^{1}H NMR, and IR spectroscopies as well as Fe^{2+}/Fe^{3+} redox potential measurements. While N70D mutant exhibited quite similar CD spectra and redox potential to those of native enzyme, the paramagnetic NMR spectrum clearly showed that the hydrogen bond between the distal His and Asp70 is not formed in the mutant. The disappearance of the splitting in the ^{1}H NMR signal of heme peripheral 8-methyl group observed in 50% H_2O/50% D_2O solution of N70D-CN suggests that the hydrogen bond between the distal His and heme-bound cyanide is also disrupted by the mutation, which was supported by the low C−N vibration frequency and large dissociation constant of the heme-bound cyanide in the mutant. Together with the results from various spectroscopies and redox potentials, we can conclude that the improper positioning of the distal His induced the cleavages of the hydrogen bonds around the distal His, resulting in the substantial decrease of the catalytic activity without large structural alterations of the enzyme. The His−Asn hydrogen bond in the distal site of peroxidases, therefore, is essential for the catalytic activity by controlling the precise location of the distal His.

Horseradish peroxidase, a prototypical hemoprotein peroxidase, catalytically oxidizes small substrates to free radical products, notably the conversion of phenol to phenoxy radical (Dunfold, 1991). The ferric state (resting state) of the enzyme reacts with hydrogen peroxide to give compound I, a two-electron oxidized species in which the heme is oxidized to a ferryl porphyrin π cation radical. The compound I is reduced back to the resting state by substrates in the two successive reactions. At first, a substrate molecule reduced the compound I to the ferryl porphyrin species termed as compound II, and subsequently, the ferryl species is reduced by another substrate to regenerate the resting state.

Peroxidase and other hemoproteins such as globins, while sharing common features of the heme active site, perform completely different chemistry. The most prominent difference from globins is the reactivity to hydrogen peroxide. Peroxidases rapidly react with hydrogen peroxide at the rate of $\sim 10^7$ M^{-1} s^{-1} (Loo & Erman, 1975), whereas metmyoglobin reacts very slowly ($\sim 10^2$ M^{-1} s^{-1}) (Yonetani & Schleyer, 1967). On the basis of the crystal structure of cytochrome *c* peroxidase (C*c*P),[1] Poulos and Kraut (1980) proposed a mechanism for the peroxidase-catalyzed heterolytic cleavage of the O−O bond in the formation of compound I. One of the essential features of this mechanism is acid−base catalysis by a distal histidine (His); the His residue located in the distal cavity of peroxidase facilitates formation of the initial Fe−OOH complex by deprotonating a hydrogen peroxide as a base and subsequently assists the heterolytic cleavage of the O−O bond by protonating to the distal oxygen as an acid (Poulos & Kraut, 1980). Recently, site-directed mutagenesis of the distal His has shown that the replacements by Leu in C*c*P (Erman et al., 1992, 1993) by Ala, Val (Newmyer & Montellano, 1995), or Leu (Rodriguez-Lopez et al., 1996a) in HRP substantially decrease the formation rate of compound I by 5−6 orders of magnitude, demonstrating that the distal His in peroxidases is the most essential amino acid for the catalytic activity.

Compared X-ray crystal structures of several peroxidases (Finzel et al., 1984; Poulos et al., 1993; Edward et al., 1993; Sundaramoorthy et al., 1994; Kunishima et al., 1994; Petersen et al., 1994; Patterson & Poulos, 1995; Schuller et al., 1996) with that of myoglobin (Takano, 1977a,b; Hubbard et al., 1990), we can find a characteristic feature in peroxidases. In peroxidases, a hydrogen bond is formed

† This work was supported by a grant-in-aid for scientific research from the Ministry of Education, Science, Culture, and Sports (07309006 to I.M.).

* To whom correspondence should be addressed. Phone: +81-75-753-5931. Fax: +81-75-751-7611. E-mail: morisima@mds.moleng.kyoto-u.ac.jp.

‡ Present address: Department of Biochemistry, School of Medicine, Keio University, Shinanomachi 35, Shinjyuku-ku, Tokyo 160, Japan.

⊗ Abstract published in *Advance ACS Abstracts,* August 1, 1997.

[1] Abbreviations: HRP, horseradish peroxidase isoenzyme C; C*c*P, cytochrome *c* peroxidase; PCR, polymerase chain reaction; SDS−PAGE, sodium dodecyl sulfate−polyacrylamide gel electrophoresis; BHA, benzhydroxamic acid; native HRP, peroxidase isolated from *horseradish,* isoenzyme C; wild-type HRP, recombinant horseradish peroxidase isozyme C expressed in *Escherichia coli*; NT-CN, cyanide-ligated native HRP; WT-CN, cyanide-ligated wild-type HRP; N70D-CN, cyanide-ligated N70D HRP mutant.

S0006-2960(97)00617-X CCC: $14.00

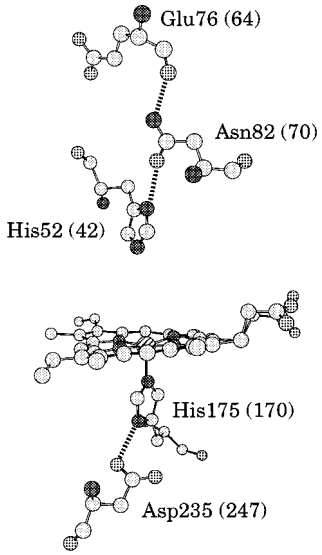

FIGURE 1: Heme and active-site residues in the X-ray crystal structure of C*c*P. Hydrogen bond is expressed as ||||||. Amino acid numbering is for C*c*P but the numbers in parentheses denote the numbering for HRP.

between the distal His and the adjacent Asn, while the corresponding hydrogen bond is not involved in myoglobin. This hydrogen bond is highly conserved in plant and fungal peroxidases (Figure 1) (Finzel et al., 1984; Poulos et al., 1993; Edward et al., 1993; Sundaramoorthy et al., 1994; Kunishima et al., 1994; Petersen et al., 1994; Patterson & Poulos, 1995; Schuller et al., 1996), suggesting that this hydrogen bond is one of the key features for the peroxidase activity. Recently, we showed that the replacement of Asn70 in HRP, which is hydrogen-bonded with the distal His, by Val (N70V) or Asp (N70D) remarkably reduced the oxidation activity for guaiacol and retarded the elementary reaction rate (Nagano et al., 1995, 1996; Mukai et al., 1997).

However, much less structural information is known for the mutant lacking the His−Asn hydrogen bond, and detailed functional regulation mechanism has not yet been clear. In order to elucidate the structure−function relationship of the His−Asn hydrogen bond in peroxidase activity, we focused here our attention on the heme environmental structure of one of the HRP N-70 mutants, N70D, since this mutants exhibited similar catalytic properties to those of another mutant, N70V (Nagano et al., 1996), which was relatively unstable. The N70D mutant also has an advantage in that its structural data can be compared with those of the corresponding C*c*P mutant, N82D (Satterlee et al., 1994). Although we have tried to crystallize these N-70 mutants to examine structural consequences, it has not yet been succeeded. Thus, in this paper, we investigated the structural features of the N70D mutant by utilizing various spectroscopies, including CD, ^{1}H NMR, and IR, and will discuss in some detail about the structure−function relationship between the highly conserved hydrogen bond in the distal site and peroxidase activity.

EXPERIMENTAL PROCEDURES

Materials. Native HRP (type VI), predominantly isozyme C, was purchased from Sigma as a lyophilized, salt-free powder and used without further purification. The A_{402}/A_{280} ratio (RZ value) of the native enzyme is 3.2. General molecular biology supplies were obtained from Takara, Toyobo, and Perkin Elmer. General organic and inorganic compounds were purchased from Wako and Nakarai Tesque.

Site-Directed Mutagenesis. Site-directed mutagenesis of the Asn70 in recombinant HRP was carried out by using the polymerase chain reaction (PCR) technique with T7 HRP as a template (Nagano et al., 1995). The synthetic oligonucleotide 5′-GCTGTTAGCGTCCCCGAATGC-3′ was used as a primer to multify double-stranded DNA fragments bearing mutation (Asn70 → Asp). The mutated DNA fragments were then ligated into the wild-type gene at 16 °C for 10 h by utilizing the unique *Nde*I and *Bgl*II restriction enzyme sites in the T7 HRP vector. We used the *Escherichia coli* strain BL 21 to transform the ligation mixture with ampicillin resistance. Positive clones yielded after an overnight incubation at 37 °C were screened by SDS−PAGE. Introduction of the mutation was verified by double-stranded DNA sequence analysis using the dideoxy chain termination method with 373 DNA sequencer (Applied Biosystems). No additional mutations were detected in the whole HRP-coding gene.

Expression, Reconstitution, and Purification of Recombinant HRP. The wild-type and mutant HRPs were expressed in *E. coli* strain BL 21 and the crude protein was extracted from inclusion bodies as described previously by Nagano et al. (1996). Reactivation of apo-HRP in the presence of calcium and heme and purification of holo-HRP were followed by the methods of Smith et al. (1990) and Gazaryan et al. (1995).

The RZ values of purified wild-type and N70D mutant are about 3.2 and 4.0, respectively. Peroxidase concentration was determined by the Soret extinction coefficient in the pyridine hemochrome form (Paul et al., 1953). These values were 102 mM^{-1} cm^{-1} for native, 103 mM^{-1} cm^{-1} for wild-type, and 125 mM^{-1} cm^{-1} for N70D mutant HRPs, respectively (Nagano et al., 1996).

Circular Dichroism (CD) Spectroscopy. CD spectra of HRPs in far-UV and Soret regions were measured with JASCO J-720 at ambient temperature. Mean residue α-helical content was evaluated from the mean residue ellipticity at 222 nm by following the eq 1 (Greenfield & Fasman, 1969):

$$\alpha\text{-helix}\ (\%) = -([\theta]_{222} + 2340)/30300 \qquad (1)$$

In the course of the measurement, nitrogen gas was purged into the cell in order to avoid incorporated chirality of dioxygen. CD spectra in this paper were an average of 16 scans recorded at a speed of 100 nm/min and a resolution of 0.2 nm. Light path of a sample was 1 mm in far-UV region and 10 mm in Soret region, respectively.

Proton Nuclear Magnetic Resonance (^{1}H NMR) Spectroscopy. ^{1}H NMR measurement was performed on a GE Omega 500 spectrometer. All the ^{1}H NMR spectra of HRPs-CN were recorded at 23.0 °C. Solutions for the ^{1}H NMR measurements were 0.5−1.0 mM (heme base) in 90% H_2O or 100% D_2O containing 50 mM sodium phosphate buffer, pH(D) 7.0. The solution pH was measured with a Beckman Model 3550 pH meter. The pD value was adjusted by using 10 N NaOD and was not corrected for the isotope effect. Sodium cyanide (10 equiv) was added to generate HRP-CN. Signal-to-noise ratio was improved by exponential apodization which introduced 10−30 Hz line broadening. Peak

shifts were referenced to the residual water signal which calibrated against tetramethylsilane (TMS).

To detect the one-dimensional nuclear Overhauser effect (1D-NOE), we used the following pulse sequence:

$$(A[t_1 - t_{on} - P - \mathrm{Acq}]_n B[t_1 - t_{off} - P - \mathrm{Acq}]_n)_m \quad (2)$$

where *A* and *B* designate two different data files, t_1 is a preparation time to allow the relaxation of the resonances (100 ms), t_{on} is the time during which the resonance is kept saturated (30 ms), and t_{off} is an equal time (30 ms) during which the decoupler is set off-resonance. *P*, the observe pulse was a Redfield 2-1-4-1-2 excitation pulse train. The NOE difference spectrum was obtained by subtracting *B* from *A*.

Fourier-Transformed Infrared (FT-IR) Spectroscopy. IR spectra were recorded on a FTS-30 spectrometer interfaced with a SPC 3200 computer (Bio-Rad) and purged with dry air. An infrared cuvette with two 13 × 22 mm CaF_2 windows separated by a 0.1 mm spacer was used for the measurement. Solutions of 1.0−1.5 mM ferric enzymes were prepared in sodium phosphate buffer, pD 7.0. The pD value was not corrected for the isotope effect. The signal-to-noise ratio was significantly improved by use of D_2O as a medium, since the absorbance by D_2O near 2100 cm^{-1} is much weaker than that by H_2O. To generate HRP-CN, *ca.* 10 equiv of sodium cyanide was added to the ferric enzyme solution and the complete formation of the CN adduct was ensured by the UV−vis spectra. We used the reference cell containing the ferric protein without cyanide. The FT-IR spectra reported here were an average of 512 scans recorded at a speed of 15 scans/min and a resolution of 1 cm^{-1}.

Cyanide and BHA Binding. UV−vis spectra of the Soret region for HRPs with various concentrations of benzhydroxamic acid (BHA) or sodium cyanide were recorded in 50 mM sodium phosphate buffer, pH 7.0. Titration was carried out at room temperature by successive additions of a BHA (0.5−50 mM) or sodium cyanide (0.5−1 mM) solution. The dissociation constants were obtained by fitting the data using a weighted least-squares error minimization procedure of the following equation corresponding to reversible binding of ligand to a single site (Smith et al., 1992).

$$A = 2A_\infty L/\{(L + K_d + P) + [(L + K_d + P)^2 - 4PL]^{1/2}\} \quad (3)$$

In the eq 3, *A* is the absorbance change at 421 nm (cyanide) or 408 nm (BHA) for a total ligand concentration *L*. A_∞ is the maximum absorbance change, and *P* is the total enzyme (binding site) concentration. All data were corrected for dilution during addition of the ligands.

Redox Potential Measurement (Fe^{2+}/Fe^{3+} Couple). Measurement of redox potential of HRP was performed with a platinum electrode and a Shimadzu MPS-2000 UV−vis spectrophotometer (Yamada et al., 1975). Safranine T, phenosafranine, benzylviologen, and α-hydroxyphenazine as mediators were added to 50 mM potassium phosphate buffer, pH 7.0, containing 50 mM EDTA (Shiro et al., 1995). The solution was allowed to sit under nitrogen atmosphere at ambient temperature for 20 min. In order to scavenge oxygen, catalase, glucose oxidase, and glucose were added with a gas-tight syringe and incubated at 20 °C for 30 min to ensure anaerobiosis. Then, *ca.* 10 μM HRP was added into the solution. The preparation of the solution described above was performed in the dark to avoid reduction of HRP by lighting during the procedure. The reductive titration of HRP was carried out with a short irradiation of white lamp. After the solution in the quartz cuvette was subjected to the irradiation for several seconds, the corresponding absorbance at 435 nm and electrode potential value were recorded. This process was repeated until HRP could not be reduced by the irradiation.

Table 1: Mean Residue Molar Ellipticities at 222 nm and Calculated α-Helical Contents of NT-CN, WT-CN, and N70D-CN

HRP-CN	$-[\theta]_{222} \times 10^{-4}$ [a]	α-helix (%)
native	1.46	40
wild-type	1.56	44
N70D	1.47	41

[a] Mean residue ellipticity in deg cm^2 $dmol^{-1}$

The midpoint potential (E_0) of HRP was obtained from the plot of the monitored electrode potential (E_h) against the percentage of reduced HRP estimated from the absorbance change at 435 nm by using the following Nernst equation:

$$E_h = E_0 + (RT/\nu F) \ln\{[\text{oxidized HRP}]/[\text{reduced HRP}]\} \quad (4)$$

where ν and *F* denote number of electrons involved in the redox reaction and Faraday constant, respectively. The midpoint potential values of HRPs were corrected by utilizing a phenosafranine (−252 mV) as a standard.

RESULTS

CD Spectroscopy. In the far-UV region, CD spectrum is composed of molar ellipticities of secondary structures. In particular, content of the α-helix structure in a protein is estimated by using the molar ellipticity at 222 nm (eq 1). The CD spectrum of N70D mutant was almost identical to those of native and wild-type HRPs (data not shown). The α-helical contents calculated from eq 1 are summarized in Table 1. No significant changes in the α-helical content was observed by the amino acid substitution at Asn70.

In the Soret region, CD spectrum provides us with unique information about interactions between heme and active site, since the chirality of the heme is induced by the interactions with chiral neighboring amino acids (Anderson & Peterson, 1995). The CD spectrum of N70D-CN in the Soret region did not exhibit a different pattern relative to those of native and wild-type enzymes (data not shown). This result indicated no apparent changes in the interactions of the heme with the apoprotein.

^{1}H NMR Spectroscopy. Figure 2 illustrates the hyperfine-shifted ^{1}H NMR spectra of WT- and N70D-CN in 90% H_2O/10% ^2H_2O (Figure 2, panels a and c) and 99% ^2H_2O (Figure 2, panels b and d) at 23.0 °C.[2] As clearly shown in the figure, the amino acid substitution of Asn70 caused upfield shifts for the heme methyl resonances. A hyperfine-shifted

[2] In the ^{1}H NMR spectra of N70D-CN (Figure 2, panels c and d), the mutant enzyme is not spectroscopically homogeneous, as exhibited by the appearance of minor resonances around 19.5 and 21.0 ppm. Since the purity of the mutant enzyme is high enough (single band in SDS−PAGE), the minor peaks might arise from the different conformer of the enzyme. Such a heterogeneity is also encountered for NMR spectra of a N82A C*c*P mutant (Alam et al., 1995).

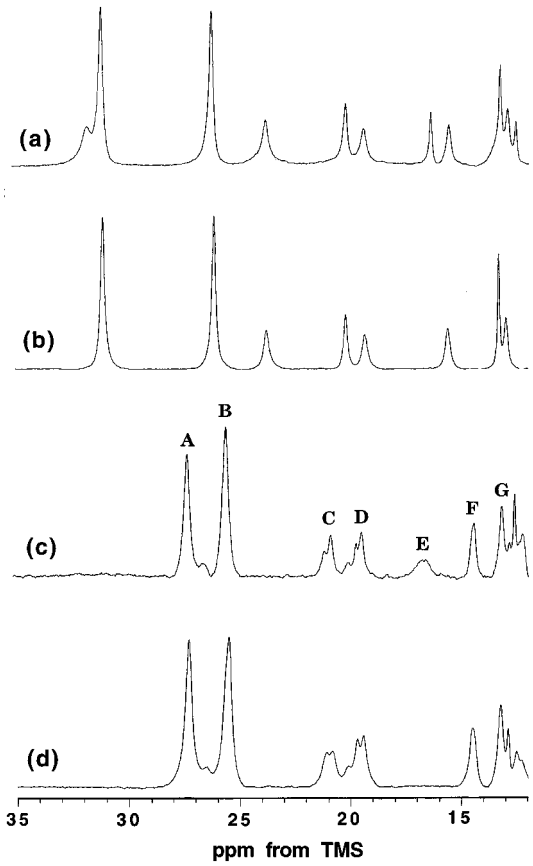

FIGURE 2: ^{1}H NMR spectra in the low-field hyperfine shift region of WT-CN (a) in 90% H_2O/10% ^2H_2O buffer and (b) in 99% ^2H_2O and N70D-CN (c) in 90% H_2O/10% ^2H_2O, (d) in 99% ^2H_2O, pH 7.0 at 23.0 °C.

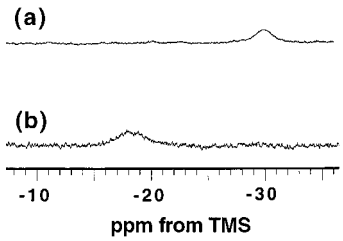

FIGURE 3: ^{1}H NMR spectra in the high-field hyperfine shift region of (a) WT-CN and (b) N70D-CN in 90% H_2O/10% ^2H_2O, pH 7.0 at 23.0 °C.

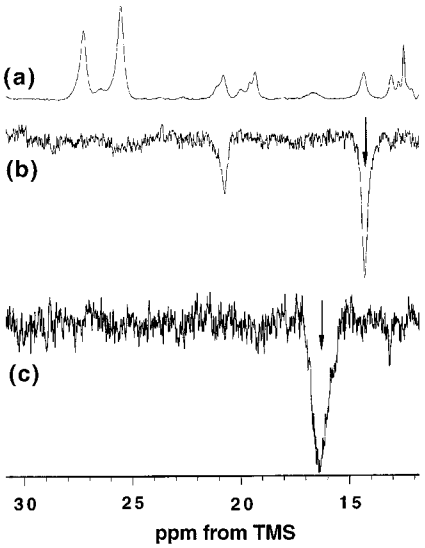

FIGURE 4: ^{1}H NMR spectra of N70D-CN in 90% H_2O/10% ^2H_2O, pH 7.0 at 23.0 °C. Spectrum a was collected with use of a Redfield 2-1-4-1-2 pulse sequence. b and c are the NOE differece spectra generated by subtracting the reference spectra with decoupler off-resonance from a similar spectrum of the same sample in which the desired resonance was saturated. In each of the difference spectra, a downward arrow indicates the peak being saturated.

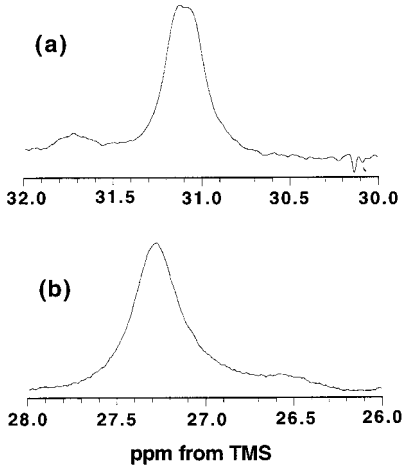

FIGURE 5: Solvent isotope effect on the heme 8-methyl resonance region in the ^{1}H NMR spectra of (a) WT-CN and (b) N70D-CN in 50% H_2O/50% ^2H_2O, pH 7.0 at 23.0 °C.

signal at 16.4 ppm, E, disappeared in the deuterated buffer (Figure 2d). The disappearance indicates that this resonance is derived from a labile proton and the peak E in N70D-CN is assignable to $N_\delta H$ of His42 (Thanabal et al., 1987). Careful comparison of the spectrum in H_2O (Figure 2c) with that in ^2H_2O (Figure 2d) reveals that the intensity of the peak B is decreased in ^2H_2O, indicating that two peaks are overlapped at 25.5 ppm in the spectrum of N70D-CN in H_2O. Since the labile proton of $N_\epsilon H$ in His42 for native enzyme appears at 31.0 ppm, the resonance of $N_\epsilon H$ in His42 for the mutant would be superimposed on the signal of 8-CH_3. In Figure 3, NMR spectra in the upfield region for wild-type (Figure 3a) and mutant (Figure 3b) are illustrated. A broadened $C_\epsilon H$ resonance of His170 in N70D-CN experienced a large downfield shift from −30.0 to −18.0 ppm by the mutation.

Figure 4 shows the Redfield ^{1}H NMR spectra of N70D-CN in 90% H_2O/10% ^2H_2O at 23.0 °C. Irradiation of the nonlabile proton peak C yields a strong NOE to a nonlabile proton peak F, suggesting the peaks of C and F are assignable to the two protons at the C_β position of His170 in the mutant (Thanabal et al., 1987). Since the saturation of the labile proton E ($N_\delta H$ of His42) yields a detectable NOE connectivity to the signal G (Figure 4c), the peak G can be assigned to the $C_\epsilon H$ resonance of His42, as shown previously in NT-CN (Thanabal et al., 1988). The signal positions and assignments of WT-CN and N70D-CN are listed in Table 2.

Figure 5 provides the 8-methyl resonances of HRPs-CN observed in 50% H_2O/50% ^2H_2O, pH 7.0. The 8-methyl resonance is split in the ^{1}H NMR spectrum of the wild-type enzyme, and Thanabal et al. (1988) ascribed the splitting to isotope effects, which reflects a significant link between the heme ligand (cyanide) and the distal His. The left and right components correspond to the states in which the N_ϵ atom of His42 possesses the proton and the deuterium, respectively (Lecomte & La Mar, 1987; Thanabal et al., 1988). In the case of N70D-CN, the corresponding split was not found in

Table 2: Chemical shifts (ppm) and Assignments of the Heme and Amino Acid Protons of NT-CN, WT-CN, and N70D-CN in Sodium Phosphate Buffer, pH 7.0 at 23.0 °C

assignment	WT-CN	N70D-CN
heme 8-CH_3	31.0	27.2
heme 3-CH_3	26.2	25.5
His170 $C_\beta H_1$	23.7	20.9
His170 $C_\beta H_2$	15.6	14.4
His170 $C_\epsilon H$	−29.9	−18.2
His42 $N_\epsilon H$	31.8	25.5
His42 $N_\delta H$	16.4	16.7
His42 $C_\epsilon H$	13.3	13.1

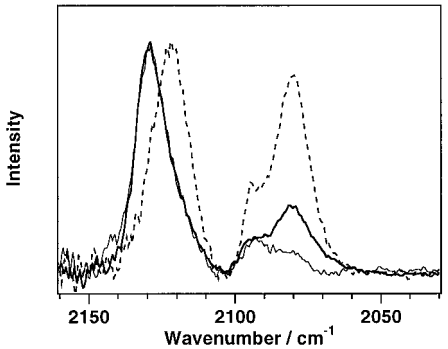

FIGURE 6: IR spectra of NT-CN (thick line), (b) WT-CN (thin line), and (c) N70D-CN (dashed line) in sodium phosphate buffer, pD 7.0.

Table 3: Dissociation Constants (K_d/μM) for the Binding of CN^- and BHA to HRPs

HRP	CN^-	BHA
native	2.7 ± 0.1	2.6 ± 0.1
wild-type	2.4 ± 0.2	2.3 ± 0.1
wild-type[a]	3	2.5 ± 0.1
N70D	3.7 ± 0.2	(9.7 ± 0.8) × 10^2
H42L[a]	30	(2.9 ± 0.5) × 10^3
R38L[a]	65	(1.21 ± 0.07) × 10^4

[a] Meunier et al. (1995) for CN^- binding and Rodriguez-Lopez et al. (1996a) for BHA binding.

the heme 8-methyl resonance, implying disruption of the hydrogen bond between His42 and heme-bound cyanide in N70D-CN.

FT-IR Spectroscopy. FT-IR measurements were applied to examine the disruption of the His42-bound cyanide hydrogen bond suggested by the solvent isotope effects on the 8-methyl resonance. Figure 6 shows FT-IR spectra of HRPs-CN. The peaks at 2130, 2094, and 2080 cm^{-1} for NT-CN have been assigned to the vibration mode of the C−N bond in the heme-bound CN, free HCN, and free CN^-, respectively (Yoshikawa et al., 1985). Recombinant WT-CN also exhibited the similar IR spectra to that of NT-CN. On the other hand, in N70D-CN, the peak of heme-bound cyanide apparently shifted to 2122 cm^{-1} (2130 cm^{-1} for NT- and WT-CN). The shift of the vibration mode to the low wavenumber side indicates that the C−N bond in heme-bound cyanide of N70D-CN is weakened by the amino acid substitution of Asn70.

Cyanide and BHA Binding. Table 3 shows dissociation constants for cyanide and BHA of HRPs. The K_d value for cyanide of wild-type HRP (2.4 μM) was in good agreement with that reported by Meunier et al. (1995) (3 μM). As listed in Table 3, a slightly but significantly larger K_d value (3.7 μM) was obtained for N70D mutant. For BHA binding, the difference between the mutant and native enzyme was enhanced. N70D mutant exhibits a much larger K_d value (9.7 × 10^2 μM) than native (2.6 μM) and wild-type (2.3 μM) HRPs (Smith et al., 1992; Rodriguez-Lopez et al., 1996a).

Table 4: Midpoint Potential of Fe^{2+}/Fe^{3+} Couple in Native, Wild-Type, and N70D HRPs

HRP	E_0/mV
native	−266
wild-type	−258
N70D	−267

Redox Potential Measurement. Redox potential of Fe^{2+}/Fe^{3+} couple was measured to examine an influence of the mutation on the proximal site, notably electronic property of the proximal His. The monitored electrode potential against the percentage of reduced HRP was fitted well by the theoretical Nernst equation (eq 4) (data not shown). The ν values of native, wild-type, and N70D HRPs were estimated as 0.90, 0.90, and 1.0, respectively, which confirmed that one electron was involved in the Fe^{2+}/Fe^{3+} redox reaction. The midpoint potentials calculated from the theoretical curves were summarized in Table 4. The redox potential (−266 mV) of native HRP was in good agreement with the value (−258 mV) reported by Yamada et al. (1975). The redox potential value of N70D (−267 mV) was also reconciled with those of native and wild-type enzymes, although the amino acid was substituted.

DISCUSSION

Hydrogen Bond Network in the Distal Cavity and Reorientation of the Distal His. Our previous reports (Nagano et al., 1995, 1996) have shown that the catalytic properties for N70D mutant were decreased as found for N70V mutant, in which the distal His cannot form a hydrogen bond to other amino acids in the distal cavity. In order to get further insight into the hydrogen bond involving the distal His, we utilized various spectroscopies for the N70D mutant. The signal width of the $N_\delta H$ resonance of His42 in the NMR spectrum of HRP-CN has served as one of the markers for the formation of hydrogen bonds between the distal His and other amino acid residues. As shown in Figure 2c, the $N_\delta H$ resonance in the distal His for N70D was substantially broadened compared to that of WT-CN. Since rapid chemical exchange of a proton gives rise to the broadening of its signal (Looney et al., 1957), we attributes the broad $N_\delta H$ resonance of His42 in N70D to rapid exchange with protons of bulk water (Cutnell et al., 1981; Thanabal et al., 1988), confirming that the hydrogen bond is not formed between the distal His and Asp70.

The hydrogen bond between the distal His and the sixth ligand of heme iron has been also considered to play a key role in the catalytic activities of peroxidases (Poulos & Kraut, 1980; Sitter et al., 1985; Dunfold, 1991). In NT-CN, Thanabal et al. (1988) reported that the chemical shift for 8-CH_3 depends on solvent isotope composition and concluded that the isotope effect reflects a hydrogen bond between the distal His and the heme ligand. In N70D mutant, however, the 8-CH_3 resonance was insensitive to the solvent isotope composition as illustrated in Figure 5, suggesting that the N_ϵ atom of His42 is not hydrogen bonded with the bound cyanide.

The lower vibration frequency of the heme-bound cyanide observed in the IR spectrum of N70D-CN also supports the disruption of the hydrogen bond. By use of model complex, Eaton and Sandercock (1982) have shown that the formation of hydrogen bonds shifts the cyanide stretching frequency to higher energy. In other words, the decrease of wavenumber in vibration frequency of iron-bound ligand is related with elimination of interaction between the ligand and a polar group. In N70D mutant, the stretching mode for C−N in the liganded cyanide shifted to the low wavenumber by 8 cm^{-1}, implying that the environment around the liganded cyanide is less polar, which corresponds to the disruption of the hydrogen bond between the distal His and the liganded cyanide. Such a disruption of the hydrogen bond is consistent with the large dissociation constant for cyanide in the mutant (Table 3).

Although N70D mutant fails to form both of the hydrogen bonds, the structural alterations are rather small. CD spectrum of the mutant is almost identical to that of the wild-type enzyme and the α-helical content is retained regardless of the amino acid replacement. As listed in Table 2, the deviations of most of the resonances from the heme methyl groups and amino acid residues near the heme iron are within 5 ppm. These spectral similarities suggest that the effects of the breakage of the hydrogen bonds are localized and the electronic structure is also unaffected by the mutation.

However, prominent large peak deviations were found in His42 (distal His) $N_\epsilon H$ (6 ppm) and His170 (proximal His) $C_\epsilon H$ (12 ppm) in the ^1H NMR spectrum of N70D-CN. Since the distal histidyl $N_\epsilon H$ would be located near the heme iron closely enough to experience the substantial pseudocontact shift to the anisotropic paramagnetic center of the heme iron as found for myoglobin (Sheard et al., 1970), the deviation of the resonance position of His42 $N_\epsilon H$ can be interpreted as the reorientation of the distal His, which is induced by the elimination of the hydrogen bond to other amino acids in the distal cavity. The reorientation of the distal His is also manifested by BHA binding in the mutant (Table 3). Addition of BHA substantially affected the NMR spectra of native HRP (La Mar et al., 1992), suggesting the formation of hydrogen bonds between BHA and the distal His. The enhancement of the dissociation of BHA in the mutant could be attributed to the disruption of the hydrogen bond, indicating the structural perturbation around the distal His.

Another NMR resonance showing the large shift by the mutation is His170 $C_\epsilon H$ in the proximal His. Since recent studies (Emerson & La Mar, 1990; La Mar et al., 1995) reported that the chemical shift of His170 $C_\epsilon H$ (Figure 3b) is substantially affected by tilt of the heme-bound cyanide, it is likely that the disruption of the hydrogen bond between the distal His and cyanide would perturb the tilt angle of the heme-bound cyanide. On the other hand, some of the previous reports pointed out that the chemical shift of the His170 $C_\epsilon H$ is also related with electronic property of the proximal His (La Mar et al., 1982; Veich et al., 1992). Decreased anionic character of the proximal His would induce the large downfield shift of the His170 $C_\epsilon H$ resonance and the smaller dispersion of the His170 $C_\beta H_2$ resonances (La Mar et al., 1982; Veich et al., 1992), as shown in Figures 2 and 3. However, the redox potential of the mutant (−267 mV), which is comparable to those of native (−266 mV) and wild-type (−258 mV) enzymes, indicates that the anionic character of His170 in the N70D mutant basically corresponds to that in native HRP (Goodin et al., 1993). The resonance positions of other protons in the proximal His did not exhibit large deviations from those of the wild-type enzyme. Thus, the preferential shift of the peak from the His170 $C_\epsilon H$ is due to the perturbation of the tilt angle of the heme-bound cyanide rather than the alterations of the electronic nature of the axial histidine residue.

On the basis of the present results of ^1H NMR spectroscopy together with IR spectroscopy and redox potential measurement, we can conclude that the hydrogen bond between the distal His and heme-bound cyanide as well as between the distal His and Asp70 is disrupted in the N70D mutant. The disruption of the hydrogen bond between the distal His and Asp70 caused the reorientation of the distal His, resulting in the successive cleavage of the hydrogen bond between Asp70 and heme-bound cyanide.

It is quite interesting here to compare the present structural data with those of the corresponding C*c*P mutant, N82D. In the previous report focused on C*c*P N82D-CN mutant, three resonances from the distal His ($N_\delta H$, $N_\epsilon H$, and $C_\epsilon H$) disappeared in the spectrum (Satterlee et al., 1995), which is clearly observed in C*c*P WT-CN. The disappearance can be ascribed to elimination of the His52−Asp82 hydrogen bond; the disruption of the hydrogen bond renders the distal His to reorient to a different direction, eventually shifting the three resonances to the upfield side in the unresolvable region of the NMR spectrum (Satterlee et al., 1995). In Figure 2, the three resonances from the distal His still appear in the hyperfine-shifted region. In marked contrast to the C*c*P N82D-CN, the small shifts observed in the resonances indicate that the replacement of Asn70 by Asp in HRP does not alter the location of the distal His so much as that in C*c*P, implying that the roles of Asn70 in HRP is somewhat different from those of the corresponding Asn82 in C*c*P. It may be related with the different polarity (Rodriguez-Lopez et al., 1996b) and amino acid sequence (Welinder, 1985; Schuller et al., 1996) in their respective distal heme pockets and resultant different electrostatic and steric interactions around the His−Asn hydrogen bond.

Structure−Function Relationship of Hydrogen Bond Network in the Distal Site of Peroxidases. In resonance Raman measurements for Fe−N_ϵ (His170) stretching vibration of ferrous HRPs (Nagano et al., 1996, Mukai et al., 1997), we observed a pH-dependent frequency shift with the midpoint pH value at 7.2 for NT-HRP and 5.5 for N70D mutant. Since the pK_a values were ascribed to the protonation of the distal His (Teraoka & Kitagawa, 1981), the decrease of the pK_a value corresponds to less basicity of the distal His in the N70D mutant. We, consequently, concluded that the smaller rate constants for the reaction with hydrogen peroxide in the mutant are attributed to the less basic distal His. In the present study, K_d value for cyanide dissociation in HRP-CN corresponds to the basicity of the distal His, since the deprotonation of hydrogen cyanide by distal His is a major factor for the cyanide binding process in myoglobin (Brancaccio et al., 1994). As listed in Table 3, the K_d value for cyanide of the N70D mutant is increased. Therefore, such a weak binding for the mutant accords with the less basicity of the distal His in the ferric mutant. These observations clearly indicate that the breakage of the hydrogen bond between the distal His and Asn70 reduced the basicity of the distal His, which led to the substantial decrease in peroxidase activity of the mutant.

Previous studies pointed out that the position of the distal His is also crucial for the peroxidase activity (Savenkova et al., 1996; Ozaki et al., 1996). The oxidation activity for guaiacol of the mutated HRP bearing the distal His at the position of 41 instead of the His42 was decreased 170-fold relative to that of native HRP (Savenkova et al., 1996). The preferential shift in the NMR signal from the distal His of the N70D mutant strongly suggests that the orientation of the distal His is affected by the elimination of the hydrogen bond between the distal His and Asn70 and that the position of the distal His in the mutant is shifted from that observed for wild-type enzyme. It should be noted that the reorientation of the distal His would disrupt the hydrogen bond between the distal His and the sixth ligand of the heme iron, which is essential for peroxidase activity. For instance, the distal His is hydrogen bonded to −OOH in compound 0 (Fe−OOH complex) (Poulos & Kraut, 1980), which has been considered to facilitate formation of compound I. In addition, the hydrogen bond between the distal His and a ferryl oxygen in compound II also increases reactivity of the compound II (Sitter et al., 1985; Makino et al., 1986; Hashimoto et al., 1986), eventually an overall peroxidase activity, since the reduction of compound II is a rate-determining step in the peroxidase cycle. Present results clearly show that the hydrogen bond between the distal His and the heme axial ligand (cyanide) is not formed in the N70D mutant due to the alteration of the position of the distal His. Therefore, we conclude that the distal His is strictly required to be located at the optimal position for the essential hydrogen bond network by the hydrogen bond to Asn70 for effective peroxidase catalysis. In other words, the hydrogen bond in the heme distal cavity improves the function of the distal His as a general acid−base catalyst by adjusting the precise location of the distal His as well as the basicity of the distal His through the His42−Asn70 hydrogen bond.

In N70D mutant, it would not be surprising if Asp70 can form a hydrogen bond with the distal His, since Asp has a carboxyl group. However, present study revealed that the distal His42 is not hydrogen bonded to Asp70. On the basis of the crystal structure of C*c*P, Asn70 in HRP forms a hydrogen bond not only with the $N_\delta H$ of the distal His but also with the peptide carbonyl oxygen of Glu64 (Figure 1), which is also highly conserved among various plant and fungal peroxidases. Therefore, it is most plausible that Asn70 is fixed at the optimal position by the Glu64−Asn70 hydrogen bond. In the N70D mutant, however, the hydrogen bond between Asp70 and Glu64 would be disrupted and the elimination of the Glu64−Asp70 interactions would cause the positional change of Asp70, resulting in the breakage of the His−Asp hydrogen bond and thereby reorientation of the distal His. Consequently, we can propose that Glu64 as well as Asn70 affects reactivity of the heme through the hydrogen bond network in the distal site, Glu64−Asn70−His42−ligand−heme. Some mutagenetic studies are now in progress to examine the role of Glu64 in our group.

In summary, ^{1}H NMR and IR spectra revealed the reorientation of the distal His in the N70D mutant, although the structural changes in the N70D mutant was smaller than that in the corresponding C*c*P mutant, N82D. These results together with the previous report on catalytic activity of the N70D mutant have demonstrated that the subtle reorientation of the distal His depresses the catalytic activity. In conclusion, the His−Asn hydrogen bond in the distal site improves the function of the distal His as a general acid−base catalyst by adjusting the precise location of the distal His.

ACKNOWLEDGMENT

We are grateful to Prof. Ryu Makino (Rikkyo University) for the redox potential measurement. We are also obliged to Prof. Yoshihito Watanabe (Institute for Molecular Science) for his fruitful discussion. M.T. was supported by Research Fellowships of Japan Society for the Promotion of Science for Young Scientists.

REFERENCES

Alam, S. L., Satterlee, J. D., Mauro, J. M., Poulos, T. L., & Erman, J. E (1995) *Biochemistry 34*, 15496−15503.

Anderson, L. A., & Peterson, J. A. (1995) *Biochem. Biophys. Res. Commun. 211*, 389−395.

Brancaccio, A., Cutruzzola, F., Allocatelli, C. T., Brunori, M., Smerdon, S. J., Wilkinson, A. J., Dou, Y., Keenan, D., Ikeda-Saito, M., Brantley, R. E., Jr., & Olson, J. S. (1994) *J. Biol. Chem. 269*, 13843−13853.

Cutnell, J. D., La Mar, G. N., & Kong, S. B. J. (1981) *J. Am. Chem. Soc. 103*, 3567−3572.

Dunfold, H. B. (1991) in *Peroxidases in Chemistry and Biology*, (Everse, J. E., Everse, K. E., & Grisham, M. B., Eds.) Vol. II, pp 1−24, CRC Press, Boca Raton.

Eaton, D. R., & Sandercock, A. C. (1982) *J. Phys. Chem. 86*, 1371−1375.

Edwards, S. L., Raag, R., Wariishi, H., Gold, M. H., & Poulos, T. L. (1993) *Proc. Natl. Acad. Sci. U.S.A. 90*, 750−754.

Emerson, S. D., & La Mar, G. N. (1990) *Biochemistry 29*, 1556−1566.

Erman, J. E., Vitello, L. B., Miller, M. A., & Kraut, J. (1992) *J. Am. Chem. Soc. 114*, 6592−6593.

Erman, J. E., Vitello, L. B., Miller, M. A., Shaw, A., Brown, K. A., & Kraut, J. (1993) *Biochemistry 32*, 9798−9806.

Finzel, B. C., Poulos, T. L., & Kraut, J. (1984) *J. Biol. Chem. 259*, 13027−13036.

Fukuyama, K., Kunishima, N., Amada, F., Kubota, T., & Matsubara, H. (1995) *J. Biol. Chem. 270*, 21884−21892.

Gazaryan, I. G., Doseeva, V. V., Galkin, A. G., & Tishkov, V. I. (1994) *FEBS Lett. 354*, 248−250.

Goodin, D. B., & McRee, D. E. (1993) *Biochemistry 32*, 3313−3324.

Greenfield, N., & Fasman, G. D. (1969) *Biochemistry 8*, 4108−4116.

Hashimoto, S., Tatsuno, Y., & Kitagawa, T. (1986) *Proc. Natl. Acad. Sci. U.S.A. 83*, 2417−2421.

Hubbard, S. R., Hendrickson, W. A., Lambright, D. G., & Boxer, S. G. (1990) *J. Mol. Biol. 213*, 215−218.

Kunishima, N., Fukuyama, K., Matsubara, H., Hatanaka, H., Shibano, Y., & Amachi, T. (1994) *J. Mol. Biol. 235*, 331−344.

La Mar, G. N., de Ropp, J. S., Chacko, V. P., Satterlee, J. D., & Erman, J. E. (1982) *Biochim. Biophys. Acta 708*, 317−325.

La Mar, G. N., Hernandez, G., & de Ropp, J. S. (1992) *Biochemistry 31*, 9158−9168.

La Mar, G. N., Chen, Z., Vyas, K., & McPherson, A. D. (1995) *J. Am. Chem. Soc. 117*, 411−419.

Lecomte, J. T. L., & La Mar, G. N. (1987) *J. Am. Chem. Soc. 109*, 7219−7220.

Loo, S., & Erman, J. E. (1975) *Biochemistry 14*, 3467−3470.

Looney, C. E., Phillips, W. D., & Reilly, E. L. (1957) *J. Am. Chem. Soc. 79*, 6136−6142.

Makino, R., Uno, T., Nishimura, Y., Iizuka, T., Tsuboi, M., & Ishimura, Y. (1986) *J. Biol. Chem. 261*, 8376−8382.

Meunier, B., Rodriguez-Lopez, J. N., Smith, A. T., Thorneley, R. N. F., & Rich, P. R. (1995) *Biochemistry 34*, 14687−14692.

Mukai, M., Nagano, S., Tanaka, M., Ishimori, K., Watanabe, Y., Morishima, I., Ogura, T., & Kitagawa, T. (1997) *J. Am. Chem. Soc. 119*, 1758−1766.

Nagano, S., Tanaka, M., Watanabe, Y., & Morishima, I. (1995) *Biochem. Biophys. Res. Commun. 207*, 417−423.

Nagano, S., Tanaka, M., Ishimori, K., Watanabe, Y., & Morishima, I. (1996) *Biochemistry 35*, 14251−14258.
Newmyer, S. L., & Montellano, P. R. O. (1995) *J. Biol. Chem. 270*, 19430−19438.
Ozaki, S., Matsui, T., & Watanabe, Y. (1996) *J. Am. Chem. Soc. 118*, 9784−9785.
Patterson, W. R., & Poulos, T. L. (1995) *Biochemistry 34*, 4331−4341.
Paul, K. G., Theorell, H., & Akesson, A. (1953) *Acta Chem. Scand. 7*, 1284−1287.
Petersen, J. F. W., Kadziola, A., & Larsen, S. (1994) *FEBS Lett. 339*, 291−296.
Poulos, T. L., & Kraut, J. (1980) *J. Biol. Chem. 255*, 8199−8205.
Poulos, T. L., Edwards, S. L., Wariishi, H., & Gold, M. G. (1993) *J. Biol. Chem. 268*, 4429−4440.
Rodriguez-Lopez, J. N., Smith, A. T., & Thorneley, R. N. F. (1996a) *J. Bioinorg. Chem. 1*, 136−142.
Rodriguez-Lopez, J. N., Smith, A. T., & Thorneley, R. N. F. (1996b) *J. Biol. Chem. 271*, 4023−4030.
Satterlee, J. D., Alam, S. L., Mauro, J. M., Erman, J. E., & Poulos, T. L. (1994) *Eur. J. Biochem. 224*, 81−87.
Savenkova, M. I., Newmyer, S. L., & Ortiz de Montellano, P. R. (1996) *J. Biol. Chem. 271*, 24598−24603.
Schuller, D. J., Ban, N., van Huystee, R. B., McPherson, A., & Poulos, T. L. (1996) *Structure 4*, 311−321.
Sheard, Y., Yamane, T., & Shulman, R. G., (1970) *J. Mol. Biol. 63*, 35−48.
Shiro, Y., Fujii, M., Isogai, Y., Adachi, S., Iizuka, T., Obayashi, E., Makino, R., Nakahara, K., & Shoun, H. (1995) *Biochemistry 34*, 9052−9058.
Sitter, A. J., Reczek, C. M., & Terner, J. (1985) *J. Biol. Chem. 260*, 7515−7520.
Smith, A. T., Santama, N., Dacey, S., Edwards, M., Bray, R. C., Thorneley, R. N. F., & Burke, J. F. (1990) *J. Biol. Chem. 265*, 13335−13343.
Smith, A. T., Sanders, S. A., Thorneley, R. N. F., Burke, J. F., & Bray, R. C. (1992) *Eur. J. Biochem. 207*, 507−519.
Sundaramoorthy, M., Kishi, K., Gold, M. H., & Poulos, T. L. (1994) *J. Biol. Chem. 269*, 32759−32767.
Takano, T. (1977a) *J. Mol. Biol. 110*, 537−568.
Takano, T. (1977b) *J. Mol. Biol. 110*, 569−584.
Taylor, J. F., & Morgan, V. E. (1942) *J. Biol. Chem. 144*, 15−20.
Teraoka, J., & Kitagawa, T. (1981) *J. Biol. Chem. 256*, 3969−3977.
Thanabal, V., de Ropp, J. S., & La Mar, G. N. (1987) *J. Am. Chem. Soc. 109*, 7516−7525.
Thanabal, V., de Ropp, J. S., & La Mar, G. N. (1988) *J. Am. Chem. Soc. 110*, 3027−3035.
Veich, N. C., Williams, R. J. P., Bray, R. C., Burke, J. F., Sanders, S. A., Thorneley, R. N. F., & Smith, A. T. (1992) *Eur. J. Biochem. 207*, 521−531.
Welinder, K. G. (1985) *Eur. J. Biochem. 151*, 497−504.
Yamada, H., Makino, R., & Yamazaki, I (1975) *Arch. Biochem. Biophys. 169*, 344−353.
Yonetani, T., & Schleyer, H. (1967) *J. Biol. Chem. 242*, 1974−1979.
Yoshikawa, S., O'Keeffe, D. H., & Caughey, W. S. (1985) *J. Biol. Chem. 260*, 3518−3528.

BI9706172